

# HAND DORSAL VEINS AND KNUCKLE SHAPE BASED AUTHENTICATION SYSTEM

Chaitanya Kommini, Kamalesh Ellanti, Harsha Ellanti  
 Dept of IT, SVEC, Tirupati, J.N.T.Univeristy, Anantapur,A.P – 517 102, India

**ABSTRACT**---This paper proposes a new approach to authenticate the individuals based on the hand dorsal vein images and the knuckle shape features. The proposed system is a fully automated and it uses a contactless, low-cost near IR imaging device to capture hand vein images. The minutiae points: vein bifurcations and vein endings, are extracted from the hand vein image and along with them knuckle points are used to perform authentication. The matching scores are generated in two stages: (i) hierarchical matching score from the four sets of triplets generated from binarized vein image (ii) the knuckle tip distances and vein map length. The weighted average of the matching scores is used to authenticate an individual. The proposed system produced satisfactory results and provides a more user friendly way of authenticating individuals.

**Keywords**---Image Processing, Biometrics, Contactless hand based authentication, knuckle shape, hand dorsal veins.

## I. INTRODUCTION

The effective and secure access control system requires reliable authentication system. The face identification is widely accepted component of biometrics and has higher user acceptance. Also the hand vein authentication is a promising component of biometrics. Fig. 1 illustrates the generic veins found on the dorsum of the hand. There are mainly two types of hand veins found on the dorsum of the hand, namely *cephalic* and *basilic*. The *basilic* veins are the group of veins attached with surface of hand. It generally consists of upper limb of the back of hand. *Cephalic* veins are the group of veins attached with the elbow of the hand. The shape of the veins changes with the change in the length of the body from childhood but it almost remains stable in adult life and so is a reliable source of authentication. The vascular system is largely affected due to change

in the nature of the body or of any disease. Diabetes, hypertension, atherosclerosis, metabolic disorders [17], and tumors [18] are some diseases which affect the vascular systems and made it thick or thin. Several other efforts have been considered to investigate the utility of hand veins in authentication systems. In the following section, we present a brief review on the related prior work which is followed by the salient features of the proposed approach investigated in this paper.

### A. EXISTING WORK

The reliability and uniqueness of the hand veins attracted many researchers towards its usage in authentication system. Thermal imaging cameras captures the patterns generated from the flow of blood in the cephalic and basilic veins and these patterns were employed in authenticating the individuals. Lin and Fan [1] have investigated the personal verification from such palm dorsal images acquired from the thermal infrared (IR) camera operating in (3.4-5) $\mu$ m range.

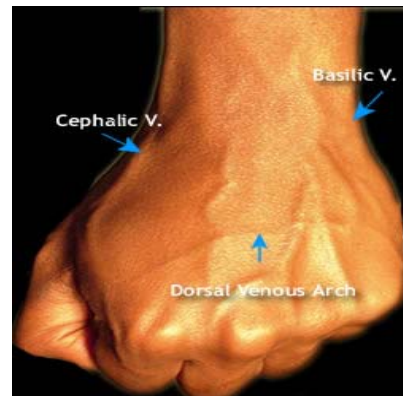


Fig. 1: Veins on the dorsum of the hand

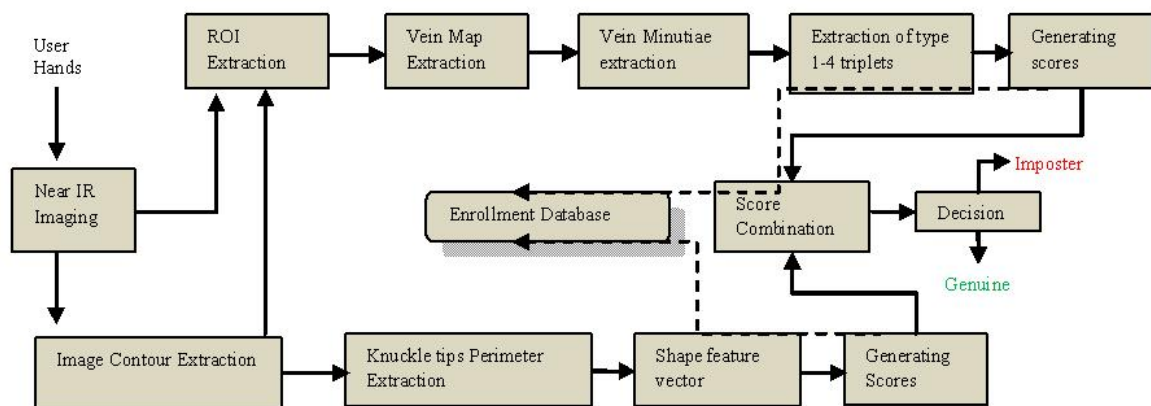


Fig. 2: Block Diagram of Hand vein and Knuckle Shape based Authentication System

The approach detailed in [1] is fully automated and uses the combination of multiresolution representations from the post processed thermal vein patterns. Wang and Leedham [2] present yet another approach for personal authentication using hand vein images acquired from the thermal imaging. Authors [2], [14] have employed Hausdorff distance to generate matching scores between the extracted line patterns and illustrated promising results. The thermal imaging cameras were usually expensive and are very sensitive to ambient conditions. But the near IR imaging produces high contrast images because of less absorption of radiation by the blood vessels. Several researchers focused on IR imaging but employed hand docking frame devices which are often inconvenient and not so user friendly. Further with notable exception there is no completely automated system for hand vein based authentication.

## B. PROPOSED WORK

In this paper, we develop a new hand vein based authentication system which utilizes the structural similarities of vein patterns and also the knuckle tips. The block diagram of the proposed approach is shown in Fig.2. This approach uses hand dorsal images acquired from low-cost, contactless, near IR imaging. The main contributions from this paper can be summarized as follows:

1. The extraction and matching of hand vein structure is done using key point triangulation. The low quality vein images do not guarantee same number of key points every time and so we use weighted combination of the key point triangulations. Further details of this strategy are discussed in section 4.
2. This system also uses knuckle shape parameters since they can be simultaneously extracted from the vein image. The matching score generated from this knuckle shapes is used to further improve the performance of the system.

The image contours extracted from the vein image are used to perform image normalizations since contactless imaging yields higher variations. The image contours are also used to extract the Region of Interest (ROI) and is discussed in sections 2-4. The automated extraction of hand vein map is detailed in section 5. The extraction and triangulation of hand vein map are discussed in sections 6-7. The hierarchical matching scheme for the triplets is introduced in Section 8. The experiments and results from this work are presented in Section 9 which is followed by the discussion in Section 10 and the main conclusions from this paper are summarized Section 11.

## II. IMAGE ACQUISITION

The acquisition of hand vein images using near IR imaging has been studied in [3], [6], and [8]. In this work, a low-cost near IR camera, traditionally used for surveillance, was employed for the contactless image acquisition. The near IR illumination (LEDs) is evenly and circularly located around the camera and peaks at 850 nm wavelength<sup>1</sup>. The expected distance between the user hand and the camera was experimentally fixed to 21 cm for the best case acquisition. The volunteers were requested to present their folded right hand (palm dorsal surface) near the imaging window such that the knuckle tip from the middle finger remains at the top. Some of

the image samples acquired from our imaging setup are reproduced in Fig. 3.

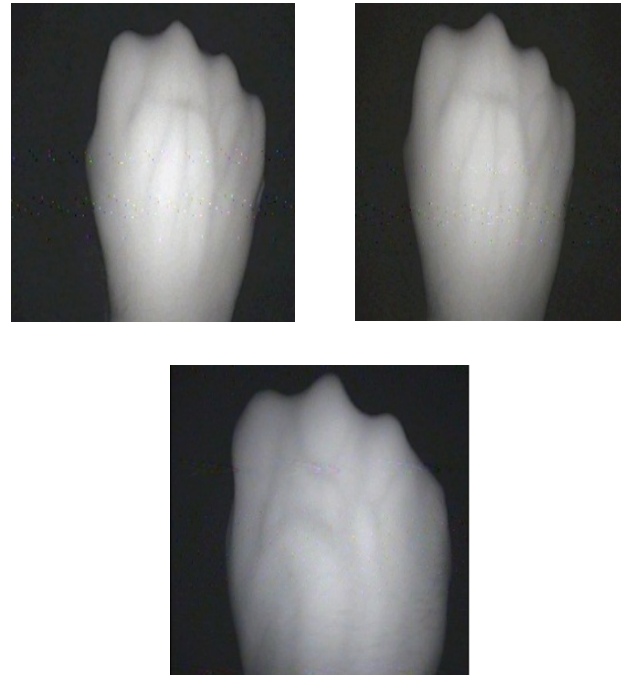


Fig 3: Samples of acquired hand images.

The incident near-infrared illumination travelling in the palm dorsal skin is absorbed by the hemoglobin in the blood and branches of artery and vein. In addition to the different absorption coefficients, the scattering coefficients of blood and bio-tissue for near infrared illumination are significantly different [34]. The higher scattering coefficient of the blood ensures that more incident infrared illumination changes its path in blood than in the surrounding tissue. It is scattering rather than absorption that dominates and results in the darker appearance of dorsal vein patterns.

## III. KNUCKLE TIPS EXTRACTION

The acquired images are firstly binarized using Otsu's thresholding and its contour is obtained as shown in Fig. 4(a). One of the key tasks in image normalization is to obtain reliable control points from the image that can be used for alignment and extraction of region of interest (ROI). In our approach, we selected knuckle tips as the control points. The knuckle tips can be easily extracted by scan the contour image from left to right and from top to bottom. The point where the first transition occurs from white to black pixel is the first knuckle tip  $\mathbf{K}_m$ . Similar scanning of the two portions of the image, i.e., left side and right side of  $\mathbf{K}_m$ , can locate index finger tip ( $\mathbf{K}_i$ ) and ring finger tip ( $\mathbf{K}_r$ ). However, as can be observed from Figs. 3 and 4 (or other images in this paper), the little finger knuckle tip (say  $\mathbf{K}_l$ ) is usually not visible and difficult to locate. In our implementation, the point is approximated contour point at the same row and column distance, as between  $\mathbf{K}_m$  and  $\mathbf{K}_r$ , from knuckle tip  $\mathbf{K}_r$  but from the aligned image contour.

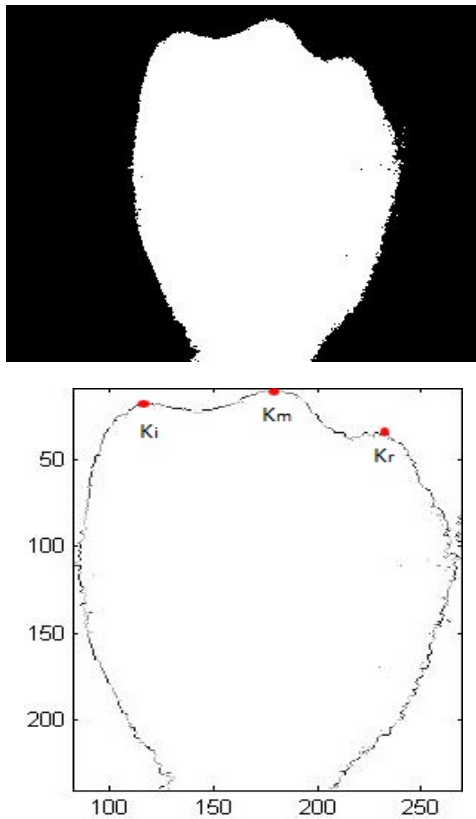


Fig 4: (a) Acquired image after thresholding and (b) Corresponding contour image with extracted key points

#### IV. EXTRACTION OF ROI

Once the key control points ( $\mathbf{K}_i$ ,  $\mathbf{K}_m$ ,  $\mathbf{K}_r$ ) are located, a fixed Region of Interest (ROI) of size 140 x 100 pixels is extracted. The size and position of this region is empirically selected and fixed at 150 pixels below  $\mathbf{K}_m$  and along the line joining  $\mathbf{K}_i$  and  $\mathbf{K}_r$ .



Fig 5: Extracted Region of Interest (ROI).

#### V. EXTRACTION OF VEIN STRUCTURE

The vein structures are extracted from the segmented Region of Interest. The images acquired from the low-cost near IR camera are of poor quality and contains obscure parts of veins due to noise and uneven illumination profile of the IR illuminators fixed at a distance. The process of extracting vein patterns is summarized in fig 6. In order to extract vein patterns, first, the images are subjected to Contrast Limited Adaptive Histogram Equalization (CLAHE) for image enhancement. Further the images are processed using Laplacian of Gaussian (LoG) or Mexican hat operator.

$$\nabla^2 G_\sigma(x, y) = \frac{1}{\pi\sigma^4} \left\{ 1 - \frac{x^2 + y^2}{2\sigma^2} \right\} e^{-\frac{x^2+y^2}{2\sigma^2}} \quad (1)$$

The LoG operator  $\nabla^2 G_\sigma(x, y)$  is used to identify the image regions with rapid intensity changes while suppressing noise. The resulting image is subjected to thinning. But the resulting also contains certain noise and so noise removal is done by eliminating the isolated regions with small amount of connectivity.

#### VI. EXTRACTION OF VEIN BIFURCATIONS AND VEIN ENDINGS

The vein bifurcation and endings points are selected as key points to extract local vein properties. A vein bifurcation is defined as vein point where vein forks or diverges into branch veins, and the vein ending is the point at which vein ends or disappears abruptly. This disappearance could be due to the abrupt ending of blood vessels or their poor visibility from the imaging system. In order to extract the vein endings and bifurcation points we examine the connectivity of every pixel and determine the crossing number  $R(\mathbf{m})$  [9] for every pixel  $\mathbf{m}$ . The crossing number  $R(\mathbf{m})$  is the sum of differences between pairs of adjacent pixels in 3 X 3 window centered at  $\mathbf{m}$ .

$$R(\mathbf{m}) = \sum_{z=1}^8 val(m_{z \bmod 8}) - val(m_{z-1}) \quad (2)$$

The pixel  $\mathbf{m}$  with  $val(\mathbf{m})=1$  is the vein ending point if  $R(\mathbf{m})=2$  and is bifurcation point if  $R(\mathbf{m}) \geq 6$ .

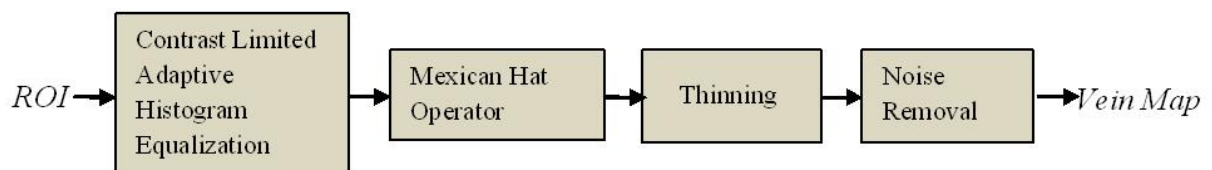


Fig 6: Extraction of Hand Vein Map from Region of Interest Images

### VII. FEATURE EXTRACTION USING MINUTIAE TRIANGULATION

The feature extraction approach is to use unique topological structure from the hand vein minutiae using Delaunay triangulation [13]. A minutiae  $M_i$  can be represented by its position and type, i.e.,  $M_i = (p_i, q_i, m_i)$  where  $(p_i, q_i)$  denotes the position and  $m_i$  denotes the type of minutiae (vein bifurcation or endings). The idea is to extract meaningful minutiae groups, i.e., triplets or triangles, from the hand vein map to achieve rotation and translation invariant representation of local information. Given a minutiae triangle (Fig. 7), we separately compute three lengths  $\lambda_1, \lambda_2$  and  $\lambda_3$ . Then all the sides of triangle are sorted to avoid considering all possible orders of same lengths

$$\lambda_1 \geq \lambda_2 \geq \lambda_3 \quad (3)$$

A 4-D index  $(\epsilon_j, \lambda_1, \lambda_2, \lambda_3)$  with  $\epsilon_j = 1,2,3,4$  is formed by indexing the triplets in the vein map. As shown in Table I, we considered four types of triplets, i.e.,  $\epsilon_j$  depending on the combinations of three types of minutiae. The number of minutiae points that can be extracted from the low quality ROI images is limited. We consider that two triplets  $Y$  and  $Y'$  are matched only if they satisfy the following set of conditions:

$$\begin{aligned} \epsilon_j = \epsilon'_j, & \quad |\lambda_1 - \lambda'_1| < T_m, \\ & \quad |\lambda_2 - \lambda'_2| < T_m, \\ & \quad |\lambda_3 - \lambda'_3| < T_m \end{aligned} \quad (4)$$

The threshold  $T_m$  can be empirically selected depending on the image size and quality.

TABLE I  
HIERARCHAL CLASSIFICATION OF TRIPLET TYPES

| TRIPLET TYPE | MINUTIAE TYPE* |          |          |
|--------------|----------------|----------|----------|
| $\epsilon_j$ | $m_1$          | $m_2$    | $m_3$    |
| 1            | <i>b</i>       | <i>b</i> | <i>b</i> |
| 2            | <i>b</i>       | <i>b</i> | <i>e</i> |
| 3            | <i>b</i>       | <i>e</i> | <i>e</i> |
| 4            | <i>e</i>       | <i>e</i> | <i>e</i> |

### VIII. SCORE ASSIGNMENT

Once the extracted triplets are matched, using the criteria in (5), the matching scores are assigned. The score assignment scheme is hierarchical and assigns higher scores to more likely true matches. If two triplets having three bifurcation points, i.e., type 1, are matched then there is higher probability that they corresponds to the same user vein map. Therefore, such matches are assigned higher scores. However, those matching triplets formed due to three vein endings, i.e., type 4, have small probability/ reliability that they have originated from the vein map of the same user. Our observations have suggested that the chances of spurious vein ending formation (due to image quality or vein extraction process) in vein map are higher. Therefore, the score assignment for such matched triplets is

the lowest (Fig. 7). The weights (or scores) are experimentally determined and such that  $w_1 > w_2 > w_3 > w_4$ . Thus, each of the matched triplet type is assigned a score and the cumulative matching score ( $S_c$ ) from all the matched triplet types is computed for every pair of hand vein matching. In addition to the usage of matching scores from the vein map (as discussed above), we also investigate the usefulness of additional features that are simultaneously extracted from the acquired images. The perimeter of pixels between four knuckle tips ( $K_i, K_m, K_r$  and  $K_l$ ) from the normalized contour image is computed. Thus, three contour distances, say  $p_1, p_2, p_3$  corresponding to distance between knuckle points  $K_i - K_m, K_m - K_r, K_r - K_l$  respectively, are also used as features. In addition, the perimeter of vein map (extracted as detailed in Section V, Fig. 6), i.e., number of white or on pixels ( $p_4$ ) are also used for the characterization of vein shape. Thus, four features ( $p_1 - p_4$ ) are used to form separate shape feature vector. The Euclidean distance between two shape features, from the two hand vein images, is used as shape matching score ( $S_g$ ). The weighted combination of two matching scores,  $S_c$  and  $S_g$ , is used compute a single consolidated matching score [35]. These consolidated matching scores are used to assign class labels (genuine or imposter) using the decision threshold.

### IX. EXPERIMENTS AND RESULTS

The performance of the proposed authentication scheme was evaluated on hand vein database acquired in the real environment. This database mainly consisted of the right hand vein images collected from the students and staff in our university. The imaging setup has been detailed in Section 2 and the size of each of the acquired images was 320 X 240.

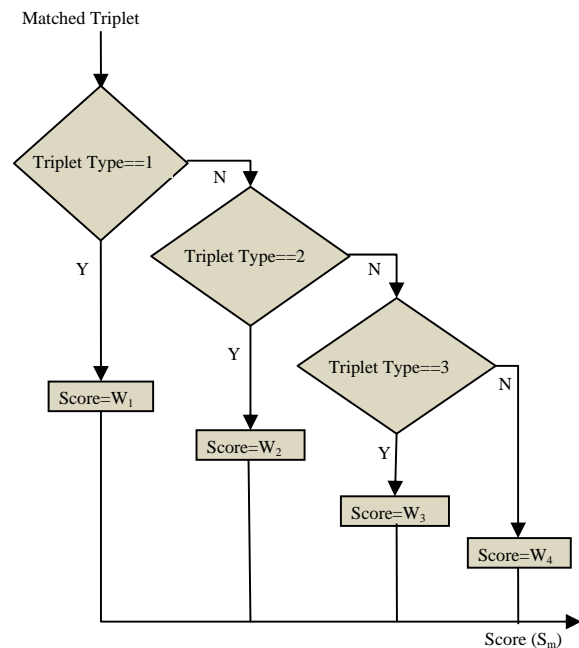


Fig 7: Score generation from a matched triplet

The ROI extraction steps detailed in Sections 3 and 4 were employed to extract 140 X 100 pixels size ROI images. These images were used to extract vein map as detailed in Section 5. The standard deviation of the 60 X 60 Mexican hat operator was empirically fixed to 0.25. The contrast limited adaptive histogram equalization was performed on 9 X 9 sub regions and matched to Rayleigh distribution with the variance of 9. All the isolated regions with 8 connected pixels and less than 100 counts were removed from the thinned images (noise removal step in Fig.6). The number of vein bifurcation points that can be extracted from the acquired images (region of interest) never exceeded 10. However, the matching scheme detailed in Section 8 has been adapted to handle the spurious vein endings. The weights from different triplet types were empirically selected as 40, 15, 8 and 3 corresponding to  $w_1, w_2, w_3$  and  $w_4$  respectively. We firstly evaluated the performance from matching scores using ( $S_c$ ) which was generated from the triplet matches. Then the performance from the geometrical features obtained from the knuckle tip distances, i.e., matching scores  $S_g$ , was integrated to ascertain the performance improvement. The weights for the combination of two matching scores,  $S_c$  and  $S_g$ , were empirically selected as 0.8 and 0.2, respectively. The equal error rate from the matching scores due to triplets alone ( $S_c$ ) is 1.77%. The equal error rate of 1.14% was achieved from the combined matching scores.

## X. DISCUSSION

The clarity and visibility of subcutaneous blood vessels varies across the user population and depends on the physiological variations, ambient temperature, humidity, hand pose, health and thickness of subcutaneous fat layer. The variation in the size and structure of venous components (e.g., lipid membrane, collagen fibers and nuclei) affect its scattering properties and alters the distribution of photon flux. In addition, the clarity of palm dorsal veins in the acquired images is also influenced by the presence of hairs, moles and scars on skin surface and also its pigmentation. Therefore, the investigated approach for the personal authentication does not depend only on the topology of venous network but also on the skin pigmentation and fat depositions on the dorsum of hand. The poor visibility of veins in the acquired images results in inaccurate extraction of venous structure and can generate spurious or missing minutiae points, which degrades the performance of the system. The average number of minutiae that that can be extracted from the low quality, i.e., poor vascular visibility and clarity, images were limited. It is interesting to note that the average number of ridge bifurcations extracted per image from our experiments was 2.81 while the average number of ridge endings observed per image was 11.53. Although the average number of ridge endings is expected to be higher than ridge bifurcations, the effect of associated noise in acquired images was observed to be more pronounced in generating spurious ridge endings than spurious bifurcations. The average number of triplets (Table I) of type 1, 2, 3, and 4 per image from our experiments were 1.53, 7.32, 12.84, and 119.82, respectively. The selection of threshold  $T_m$  in (4) is a judicious compromise between two key considerations. The larger values of threshold  $T_m$  require large number of triplets to be matched and, therefore, increase the

computational complexity. On the other hand, smaller values of  $T_m$  are also not desirable as they limit the genuine matches from the hand vein images with nonlocal deformations.

## XI. CONCLUSION

This paper has proposed a new approach for the hand authentication using vein triangulation. In addition, the unique knuckle point perimeter distances were also simultaneously extracted from the same image and utilized to achieve the performance improvement. The utility of knuckle shape biometric has been cited in [5] but there has been negligible attention on its usage in the biometric literature [6]. The illustrated performance should be interpreted in the context of contactless imaging as such images are expected to present higher intraclass variations as compared to those acquired from fixed imaging using hand docking devices. The contactless imaging is perceived to be more hygienic and user friendly but it poses problems of missing or spurious vein minutiae points. This is mainly due to the resulting uneven illumination and the fact that the palm back surface is 3-D curved surface. The hierarchical weighting of triplets is, therefore, suggested to achieve better matching performance from such images. The imaging setup employed in our work has been developed for the cooperative users in the indoor environment. It makes an assumption that user is keen to authenticate himself/herself for access and not yet suitable for the uncooperative user. The strong near IR component present in the sunlight also limits the usage of employed imaging setup for outdoor usage. The background during the indoor imaging can be controlled and can be conveniently made uniform. Our current imaging setup employs fixed focus and cannot accommodate large changes in the imaging distance. However, inclusion of auto-focus in the imaging setup can help to accommodate large changes in the imaging distance/scale. *Although more work remains to be done, our results to date indicate that the combination of hand vein and knuckle shape features constitutes a promising addition to the biometrics based personal authentication.* It is encouraging that the performance from such palm-dorsal images, using unconstrained and low-cost image setup, compares very well (or better) with the hand-geometry biometric which is has very high user acceptance [6]. While hand-geometry biometric is highly prone to spoofing, vascular biometric like palm dorsum vein are extremely difficult to forge and at the same time have high user acceptance for its deployment in civilian applications. Further improvement in the performance of proposed system, that simultaneously combines knuckle shape and dorsal vein features, using auto-focus and more sensitive near infrared camera is expected and requires further investigation. The discretization of noisy biometric features has been recently shown to offer significant improvement in the performance. This is especially useful for low-resolution imaging, such as hand geometry or the hand vein employed in this work, and is suggested for further work.

## XII. REFERENCES

- [1]. C.-L. Lin and K.-C. Fan, "Biometric verification using thermal images of palm-dorsa vein patterns," *IEEE Trans. Circuits Syst. Video Technol.*, vol. 14, no. 2, pp. 199-213, Feb. 2004.
- [2]. L. Wang and G. Leedham, "A thermal hand-vein pattern verificationsystem," in *Pattern Recognition and Image Analysis*, S.

- Singh, M. Singh, C. Apte, and P. Perner, Eds. New York: Springer, 2005, vol. 3687, pp. 58–65.
- [3]. J. Mehnert, J. M. Cross, and C. L. Smith, "Thermal graphic imaging: Segmentation of the subcutaneous vascular network of the back of the hand," Research Rep., Edith Cowan Univ., Australian Inst. Security Appl. Technol., Perth, Western Australia, 1993.
- [4]. S. Z. Li, R. Chu, S. Liao, and L. Zhang, "Illumination invariant face recognition using near-infrared images," *IEEE. Tran. Pattern Anal. Mach. Intell.*, vol. 29, no. 4, pp. 627–639, Apr. 2007.
- [5]. Colbert, "Knuckle Profile Identity Verification System," U.S. Patent, 5,862,246, Jan. 1999.
- [6]. S. Zhao, Y. Wang, and Y. Wang, "Biometric verification by extracting hand vein patterns from low-quality images," in *Proc. 4th ICIG*, Aug. 2007, pp. 667–671.
- [7]. [Online] Available: <http://www.viewse.com.cn/ProductOne.asp?ID=106>
- [8]. L. Wang and G. Leedham, "Near- and far-infrared imaging for vein pattern biometrics," in *Proc. IEEE Int. Conf. Video Signal Based Surveillance*, Sydney, Nov. 2006, pp. 52–57.
- [9]. Maltoni, D. Maio, A. K. Jain, and S. Prabhakar, *Handbook of fingerprint Recognition*. New York: Springer, 2003.
- [10]. S. Fantini and M. A. Franceschini, *Handbook of Optical Biomedical Diagnostics*. Bellingham, WA: SPIE, 2002.
- [11]. *Handbook of Biometrics*, A. K. Jain, P. Flynn, and A. Ross, Eds. New York: Springer, 2007.
- [12]. Oden, A. Ercil, and B. Buke, "Combining implicit polynomials and geometric features for hand recognition," *Pattern Recognit. Lett.*, vol. 24, pp. 2145–2152, 2003.
- [13]. G. Bebis, T. Deaconu, and M. Georgiopoulos, "Fingerprint identification using Delaunay triangulation," in *Proc. Int. Conf. Information Intelligence and Systems*, 1999, pp. 452–459.
- [14]. L. Wang, G. Leedham, and S.-Y. Cho, "Minutiae feature analysis for infrared hand vein pattern biometrics," *Pattern Recognit.*, vol. 41, no. 3, pp. 920–929, 2008.
- [15]. P. Buddaharaju, I. Pavlidis, P. Tsiamyrtzis, and M. Bazakos, "Physiology- based face recognition in the thermal infrared spectrum," *IEEE. Tran. Pattern Anal. Mach. Intell.*, vol. 29, no. 4, pp. 613–626, Apr. 2007.
- [16]. W. Norman, the Anatomy Lesson [Online]. Available: <http://home.comcast.net/~wnor>
- [17]. O. A. Carretero, "Vascular remodeling and the kallikrein-kinin System," *J. Clin. Invest.*, vol. 115, pp. 588–591, Mar. 2005.
- [18]. P. Carmeliet and R. K. Jain, "Angiogenesis in cancer and other diseases," *Nature*, vol. 407, pp. 249–257, 2000.
- [19]. J.-G. Wang, W.-Y. Yau, A. Suwandy, and E. Sung, "Person recognition by palmprint and palm vein images based on 'Laplacianpalm' representation," *Pattern Recognit.*, vol. 41, pp. 1531–1544, 2008.
- [20]. K. R. Park and J. Kim, "A real-time focusing algorithm for iris recognition camera," *IEEE Trans. Syst. Man Cybern. C*, vol. 35, pp. 441–444, Aug. 2005.